Pheophytinase knockdown impacts carbon metabolism and nutraceutical content under normal growth conditions in tomato

Lira, Bruno Silvestre ; Rosado, Daniele ; Almeida, Juliana ; de Souza, Amanda Pereira ; Buckeridge, Marcos Silveira ; Purgatto, Eduardo ; Guyer, Luzia ; Hörtensteiner, Stefan ; Freschi, Luciano ; Rossi, Magdalena

Abstract: Although chlorophyll (Chl) degradation is an essential biochemical pathway for plant physiology, our knowledge regarding this process still has unfilled gaps. Pheophytinase (PPH) was shown to be essential for Chl breakdown in dark-induced senescent leaves. However, the catalyzing enzymes involved in pigment turnover and fruit ripening-associated degreening are still controversial. Chl metabolism is closely linked to the biosynthesis of other isoprenoid-derived compounds, such as carotenoids and tocopherols, which are also components of the photosynthetic machinery. Chls, carotenoids and tocopherols share a common precursor, geranylgeranyl diphosphate, produced by the plastidial methylerythritol 4-phosphate (MEP) pathway. Additionally, the Chl degradation-derived phytol can be incorporated into tocopherol biosynthesis. In this context, tomato turns out to be an interesting model to address isoprenoid-metabolic cross-talk since fruit ripening combines degreening and an intensely active MEP leading to carotenoid accumulation. Here, we investigate the impact of PPH deficiency beyond senescence by the comprehensive phenotyping of SlPPH-knockdown tomato plants. In leaves, photosynthetic parameters indicate altered energy usage of excited Chl. As a mitigatory effect, photosynthesis-associated carotenoids increased while tocopherol content remained constant. Additionally, starch and soluble sugar profiles revealed a distinct pattern of carbon allocation in leaves that suggests enhanced sucrose exportation. The higher levels of carbohydrates in sink organs down-regulated carotenoid biosynthesis. Additionally, the reduction in Chl-derived phytol recycling resulted in decreased tocopherol content in transgenic ripe fruits. Summing up, tocopherol and carotenoid metabolism, together with the antioxidant capacity of the hydrophilic and hydrophobic fractions, were differentially affected in leaves and fruits of the transgenic plants. Thus, in tomato, PPH plays a role beyond senescence-associated Chl degradation that, when compromised, affects isoprenoid and carbon metabolism which ultimately alters the fruit's nutraceutical content.

DOI: https://doi.org/10.1093/pcp/pcw021

(2016). Pheophytinase knockdown impacts carbon metabolism and nutraceutical content under normal growth conditions in tomato. Plant Cell Physiology, 57(3):642-653.
DOI: https://doi.org/10.1093/pcp/pcw021

OXFORD UNIVERSITY PRESS | Plant and Cell Physiology

Pheophytinase knockdown impacts carbon metabolism and nutraceutical content under normal growth conditions in tomato

Journal:	*Plant and Cell Physiology*
Manuscript ID	PCP-2015-E-00700.R1
Manuscript Type:	Regular Paper
Date Submitted by the Author:	n/a
Complete List of Authors:	Lira, Bruno; University of São Paulo, Departamento de Botânica Rosado, Daniele; University of São Paulo, Departamento de Botânica Almeida, Juliana; University of São Paulo, Departamento de Botânica de Souza, Amanda; University of São Paulo, Departamento de Botânica Buckeridge, Marcos; University of São Paulo, Departamento de Botânica Purgatto, Eduardo; University of São Paulo, Departamento de Alimentos e Nutrição Experimental Guyer, Luzia; University of Zurich, Institute of Plant Biology Hoertensteiner, Stefan; University of Zurich, Institute of Plant Biology Freschi, Luciano; University of São Paulo, Departamento de Botânica Rossi, Magdalena; University of São Paulo, Department of Botany
Keywords:	Solanum lycopersicum, tomato, pheophytinase, tocopherol, carotenoids, chlorophyll degradation

Title: Pheophytinase knockdown impacts carbon metabolism and nutraceutical content under normal growth conditions in tomato

Running head: Metabolic alterations in *SlPPH*-knockdown tomato

Corresponding Author Information:

Name: Magdalena Rossi

Address: Departamento de Botânica, Instituto de Biociências, Universidade de São Paulo, Rua do Matão, 277, 05508-900, São Paulo, Brasil.

Phone: 55-11-3091-7556

Fax: 55-11-3091-7547

E-mail: mmrossi@usp.br

Subject area: Growth and Development

Total Figures: 7

Colour Figures: Fig. 1 and Fig. 3

Black and White Figures: Fig. 2, Fig. 4, Fig. 5, Fig.6 and Fig. 7

Tables: 3

Supplementary Figures: 5

Supplementary Tables: 4

Title: Pheophytinase knockdown impacts carbon metabolism and nutraceutical content under normal growth conditions in tomato

Running head: Metabolic alterations in *SlPPH*-knockdown tomato

Bruno Silvestre Lira [1], Daniele Rosado [1], Juliana Almeida [1], Amanda Pereira de Souza [1], Marcos Silveira Buckeridge [1], Eduardo Purgatto [2], Luzia Guyer [3], Stefan Hörtensteiner [3], Luciano Freschi [1], Magdalena Rossi [1*].

[1] Departamento de Botânica, Instituto de Biociências, Universidade de São Paulo, São Paulo, SP, Brazil.

[2] Departamento de Alimentos e Nutrição Experimental, Faculdade de Ciências Farmacêuticas, Universidade de São Paulo, São Paulo, SP, Brazil.

[3] Institute of Plant Biology, University of Zurich, Zurich, Switzerland.

* Corresponding Author.

Abstract

Although chlorophyll (Chl) degradation is an essential biochemical pathway for plant physiology, our knowledge regarding this process retains unfilled gaps. Pheophytinase (PPH) was shown to be essential for Chl breakdown in dark-induced senescent leaves. However, the catalyzing enzymes involved in pigment turnover and fruit ripening-associated degreening are still controversial. Chl metabolism is closely linked to the biosynthesis of other isoprenoid-derived compounds, such as carotenoids and tocopherols, which are also components of the photosynthetic machinery. Chls, carotenoids and tocopherols share a common precursor, geranylgeranyl diphosphate, produced by the plastidial methylerythritol 4-phosphate (MEP) pathway. Additionally, the Chl degradation-derived phytol can be incorporated into tocopherol biosynthesis. In this context, tomato turns out as an interesting model to address isoprenoid-metabolic crosstalk since fruit ripening combines degreening and an intensely active MEP leading to carotenoid accumulation. Here, we investigate the impact of PPH deficiency beyond senescence by the comprehensive phenotyping of *SlPPH*-knockdown tomato plants. In leaves, photosynthetic parameters indicate altered energy usage of excited Chl. As a mitigatory effect, photosynthesis-associated carotenoids increased while tocopherol content remained constant. Additionally, starch and soluble sugar profiles revealed a distinct pattern of carbon allocation in leaves that suggests enhanced sucrose exportation. The higher levels of carbohydrates in sink organs downregulated carotenoid biosynthesis. Additionally, the reduction in Chl-derived phytol recycling resulted in decreased tocopherol content in transgenic ripe fruits. Concluding, tocopherol and carotenoid metabolisms, together with the antioxidant capacity of the hydrophilic and hydrophobic fractions, were differentially affected in leaves and fruits of the transgenic plants. Thus, in tomato, PPH plays a role beyond senescence-associated Chl degradation that, when compromised, affects isoprenoid and carbon metabolisms that, ultimately, alters the fruit's nutraceutical content.

Keywords: *Solanum lycopersicum*; tomato; pheophytinase; tocopherol; carotenoids; chlorophyll degradation.

Introduction

Photosynthesis, the process on which life relies upon, converts light energy by coupling chlorophyll (Chl) with an electron transport chain. The extention of photosynthetic activity for longer periods, by delaying leaf senescence, might lead to carbon assimilation improvement. Thus, this phenotype, called stay green, has been considered as strategy for yield breeding (Rossi et al. 2015) and has been classified as cosmetic or functional (Thomas and Howarth 2000). Genotypes with deficiency in senescence-associated Chl degradation are considered cosmetic, since the non-visible components of senescence are mostly unaffected (Thomas and Ougham 2014). This seems to be the case in the *Arabidopsis thaliana* pheophytinase (*AtPPH*) mutant (*pph-1*). Pheophytinase (PPH) catalyzes the dephytylation of pheophytin *a* releasing phytol, the Chl lipophilic chain. *pph-1* is unable to degrade chlorophyll and the functionality of photosynthesis is strongly affected upon senescence induction (Schelbert et al. 2009). Similar results have been obtained for the *Solanum lycopersicum* ortholog gene, *SlPPH* (Guyer et al. 2014), as Chl breakdown is impaired in dark-induced senescent leaves of *SlPPH*-knockdown plants. The fruits of transgenic lines showed a transient delay of Chl degradation that was accompanied by a transitory accumulation of pheophytin *a*, but, ultimately, they degraded chlorophyll and pheophytin *a* like the wild type genotype. These results demonstrate the involvement of SlPPH in ripening-associated degreening, however, they also indicate that other dephytylating activities may compensate the reduced levels of PPH in transgenic fruits.

Another elusive mechanism regarding Chl metabolism is Chl turnover. It has been demonstrated that chlorophyll synthase re-esterifies chlorophyllide *a*, nevertheless the enzyme responsible for the hydrolysis of the ester bond yielding chlorophyllide *a* and free phytol is still missing (Lin et al. 2014, Zhang et al. 2015). Pheophytin *a* and Chl *a* exclusively differ in one magnesium ion, thus, it seems likely that the de-esterification is catalyzed by a PPH-like enzyme. Interestingly, pheophytin *a* recycling might also be needed for proper photosystem turnover as it is known to be the primary electron acceptor in PSII (Vass and Cser 2009). Furthermore, *PPH*-like genes are found from cyanobacterial to angiosperm genomes and have been shown to be localized in plastids (Schelbert et al. 2009, Guyer et al. 2014).

Chl metabolism is closely linked to carotenoid and tocopherol biosynthesis, which are the major lipid-soluble antioxidants of the thylakoid membrane and consequently, important players in photosynthetic activity maintenance (Havaux et al. 2005). These isoprenoid-derived compounds are synthesized from geranylgeranyl

diphosphate (GGPP) produced by the plastidial methylerythritol 4-phosphate (MEP) pathway (DellaPenna and Pogson 2006) (Fig. 1). While GGPP is the substrate for the first enzyme of carotenoid biosynthesis, phytoene synthase (PSY), the Chl and tocopherol prenyl side chain derives from phytyl diphosphate (PDP), which in turn is produced by geranylgeranyl reductase (GGDR) (Almeida et al. 2015a). Tocopherols, which belong to the vitamin E (VTE) family of compounds, are further synthesized from the condensation of PDP and homogentisate from the plastidial shikimate (SK) pathway (Almeida et al. 2011). Additionally, PDP for tocopherol biosynthesis can also originate from the activity of phytol kinase (VTE5) and phytyl-phosphate kinase (VTE6), which recycle Chl degradation-derived phytol (Ischebeck et al. 2006, Valentin et al. 2006, Almeida et al. 2015b, vom Dorp et al. 2015).

Although Chl, tocopherols and carotenoids share a common precursor, few studies have provided comprehensive insight into the regulation of their metabolic network (Quadrana et al. 2013, Almeida et al. 2015a, Zhang et al. 2014, Zhang et al. 2015). It has been demonstrated that STAY GREEN 1 (SlSGR), a Chl degradation regulatory protein, controls lycopene and β-carotene accumulation by interacting directly with SlPSY1 during tomato ripening (Luo et al. 2013). Recent evidences indicate that PDP for tocopherol biosynthesis is mostly supplied by chlorophyll degradation (Zhang et al. 2015). In seeds of *A. thaliana* neither PPH nor chlorophyllases, the other known Chl dephytylating enzyme, seem to be responsible for producing Chl-derived phytol for tocopherol biosynthesis, although *AtPPH*-overexpressing lines displayed increased levels of tocopherol (Zhang et al. 2014). Altogether, these data suggest the existence of an unknown source of phytol for tocopherol biosynthesis as well as a still obscure complex regulatory network of isoprenoid-derived compounds.

Tomato (*Solanum lycopersicum*) turns out as an interesting model to address the above described isoprenoid-metabolic crosstalk since, during fruit ripening, chloroplast-to-chromoplast transition combines degreening and an intensely active MEP leading to carotenoid accumulation (Egea et al. 2011, Barsan et al. 2012, Seymour et al. 2013); while total tocopherol content remains constant (Quadrana et al. 2013). Moreover, tomato is one of the most consumed fruits worldwide and is a major source of these nutraceutical compounds for human diet (Canene-Adams et al. 2005, Chun et al. 2006).

In this work, we further characterized *SlPPH*-knockdown plants to address the role of PPH in Chl, carotenoid and tocopherol homeostasis and the physiological impact of PPH deficiency beyond senescence. The transgenic plants showed altered photosynthetic parameters that were reflected in modifications in carbon partitioning.

Carotenoid and tocopherol content and composition were differently affected in leaves and fruits of *SlPPH*-knockdown plants, what could be explained by the transcriptional profile of respective biosynthetic genes as well as by the influence of sugars over carotenoid metabolism. In addition, antioxidant activities in both organs were altered in accordance with carotenoid and tocopherol contents. Finally, a comprehensive survey of the tomato genome revealed the presence of three other *PPH*-like genes. The transcriptional profiles suggested that they all might play a role in leaf Chl metabolism, while *SlPPHL3* could in addition be involved in ripening-associated degreening. The integrated data analysis showed that SlPPH deficiency affects isoprenoid metabolism in an organ-specific manner modifying the nutritional content of the edible fruit.

Results

Isoprenoid-derived compounds and Trolox Equivalent Antioxidant Capacity (TEAC) profiles are altered in SlPPH-knockdown plants

Aiming to investigate the effect of PPH deficiency in the metabolism of carotenoids and tocopherol, three independent *SlPPH*-knockdown lines, with at least 85% reduction of *SlPPH* mRNA level (Supplementary Fig. S1), were characterized.

Linear (lycopene) and cyclized (β-carotene, lutein, violaxanthin and neoxanthin) carotenoids were measured (Table 1). In leaves, all detected carotenoids were increased in a statistically significant manner, except for lutein that remained unaltered. On the other hand, a contrasting scenario was found in fruits. While no significant changes were found at the mature green stage, ripe fruits of *SlPPH*-knockdown plants showed reduced carotenoid levels compared to the control genotype. Again, lutein was the only measured compound that showed similar levels to wild type fruits.

Similar to that described for carotenoids, distinct tocopherol profiles were observed between organs. The levels of α-, γ- and total-tocopherol in leaves of *SlPPH*-knockdown plants were similar to those observed in the wild type; however, the transgenic lines also presented detectable amounts of δ-tocopherol. Mature green fruits of the transgenic plants accumulated higher levels of α- and γ-tocopherol, which resulted in about 12% increase in total-tocopherol content. At the ripe stage, the amount of total tocopherol decreased in *SlPPH*-

knockdown lines as consequence of the reduction of the minor tocopherol forms, γ- and δ-, whose extent was not compensated by the increment in α-tocopherol (Table 2).

As *SlPPH*-knockdown affected the profile of tocopherols and carotenoids, the antioxidant capacity in leaf and fruit extracts was estimated by the TEAC assay. The hydrophilic fraction of leaves and ripe fruits showed increased TEAC in transgenic plants, while reduced levels were detected at the mature green stage (Fig. 2A). In terms of antioxidant capacity of the lipophilic fraction, leaves of *SlPPH*-knockdown plants did not differ significantly from the wild type genotype. Interestingly, fruit TEAC profile in the non-polar extract of transgenic lines displayed the opposite pattern observed in the hydrophilic fraction (Fig. 2B).

These data indicate that the metabolism of isoprenoid-derived compounds as well as the antioxidant capacity is differentially adjusted in response to SlPPH deficiency in leaves and fruits.

SlPPH deficiency alters the transcript profile of tocopherol and carotenoid biosynthetic enzyme encoding genes.

To address whether the alterations in tocopherol and carotenoids contents observed in transgenic plants are explainable by a transcriptional regulation of respective biosynthetic genes, the mRNA levels of isoprenoid metabolism-related genes (Fig. 1) were profiled in leaves and fruits (Fig. 3 and Supplementary Table S1).

Due to the role of STAY GREEN 1 protein (SGR) in chlorophyll catabolic enzyme recruitment (Sakuraba et al. 2012) and carotenoid biosynthesis regulation (Luo et al. 2013), the transcript profile of *SlSGR* was also evaluated. Interestingly, while no effect was found in leaves and mature green fruits, significantly lower amounts of *SlSGR* mRNA were detected at breaker and ripe stages of *SlPPH*-knockdown fruits. PHEOPHORBIDE *a* OXYGENASE (PAO) is another member of the chlorophyll catabolic enzyme complex (Sakuraba et al. 2012), and the *SlPAO* also showed reduced levels of mRNA in *SlPPH*-knockdown plants in leaves and fruits indicating that these plants are, in some extent, also impaired in the tetrapyrrole ring breakdown. In *A. thaliana* the overexpression and silencing of *AtSGR1* resulted in higher and lower amounts, respectively of *AtPPH* mRNA (Sakuraba et al. 2014). Reciprocally, the results presented here showed that the reduced expression of *SlPPH* leads to the downregulation of *SlSGR* and *SlPAO* suggesting the existence of transcriptional co-regulation of the members of the Chl catabolic enzyme complex.

During tomato fruit ripening the expression of 1-DEOXY-D-XYLULOSE-5-P SYNTHASE encoding gene (*SlDXS*) increases while the amount of transcripts of the GERANYLGERANYL DIPHOSPHATE REDUCTASE encoding gene

(*SlGGDR*) diminishes. These changes in the transcriptional profile enhance the availability of isoprenoid intermediates for fruit carotenoid accumulation (Quadrana et al. 2013, Almeida et al. 2015a). Interestingly, the fruits of the transgenic plants showed a reversed pattern of expression displaying higher and lower levels of transcripts for *SlGGDR* and *SlDXS*, respectively. Conversely, the leaves of the *SlPPH*-knockdown plants showed increased amounts of mRNA for *SlDXS.*

Carotenoid metabolism was addressed by profiling the transcript amount of *PHYTOENE SYNTHASE* (*SlPSY1* and *SlPSY2*), *PHYTOENE DESATURASE* (*SlPDS*) and *LYCOPENE β-CYCLASE* (the chloroplast-specific *SlLCYβ* and the chromoplast-specific *SlCYCβ*) genes. It is worth mentioning that in chloroplast of wild type plants, both *SlPSYs* and *SlLCYβ* are highly expressed contributing to the biosynthesis of photosynthesis-associated carotenoids. In fruits, *SlPSY2* expression is insignificant while, *SlCYCβ* is the most abundant *LYCOPENE β-CYCLASE* being 7-fold more expressed than *SlLCYβ* (Supplemental Table S2). As an overall pattern, *SlPPH* silencing led to the downregulation of the analyzed genes with the exception of *SlLCYβ* at breaker and ripe stages.

The mRNA levels of tocopherol biosynthetic (*SlVTE1, SlVTE2, SlVTE3(1), SlVTE3(2)* and *SlVTE4*) and phytol recycling (*SlVTE5* and *SlVTE6*) enzyme encoding genes were also evaluated. In comparison to the control genotype, leaves of transgenic plants displayed reduction in *SlVTE4* and *SlVTE3(2)* expression, whereas in breaker fruits S*lVTE2*, *SlVTE4* and *SlVTE5* showed lower levels of transcript amounts. The later was also reduced at the mature green stage in *SlPPH*-deficient plants. Moreover, reduced amounts of mRNAs for *SlVTE6* were also observed in breaker and ripe fruits of *SlPPH*-knockdown plants compared to controls.

These data showed that *SlPPH* silencing alters the expression of several isoprenoid metabolism-related genes in leaves and fruits reinforcing the tight link between Chl, carotenoid and tocopherol metabolisms.

SlPPH-knockdown affects photosynthesis and primary carbon metabolism

Given that SlPPH deficiency led to significant changes in carotenoid and tocopherol content, the effect on plant growth and photosynthesis was also evaluated.

The height and node number data were monitored during thirteen weeks of growth and, although some transitory changes in plant height were observed until the ninth week, shoot growth in *SlPPH*-knockdown lines was largely similar to wild type plants (Supplementary Fig. S2).

Regarding Chl content, no significant alterations were identified in source leaves, mature green and ripe fruits. However, age-induced senescent leaves and petioles had impaired Chl degradation in transgenic lines (Supplementary Fig. S3).

Photosynthetic parameters were evaluated in source leaves of 7-week-old plants (Table 3). *SlPPH* silencing did not affect respiration (R_d), transpiration (E), conductance (g_s) and dark-adapted PSII maximum quantum efficiency (*Fv/Fm*). However, reduction in CO_2 assimilation (A), proportion of open PSII centers (*qP*), PSII operating efficiency (Φ_{PSII}) and electron transport rate (ETR), as well as increase in non-photochemical quenching (NPQ) were detected in comparison to the wild type. These results implied that reduced transcript levels of *SlPPH* alter the energy usage of excited Chl.

Starch and soluble sugar composition was further evaluated in *SlPPH*-knockdown plants (Fig. 4). In leaves, the allocation of fixed carbon as starch diminished whereas sucrose and glucose accumulated at higher levels. In fruits, sucrose was remarkably increased in transgenic plants in all three stages analyzed. Additionally, breaker fruits of *SlPPH*-knockdown plants showed higher levels of starch and glucose; whereas higher glucose and fructose amounts were detected in ripe fruits of most transgenic lines. The starch and soluble sugar profile revealed an altered pattern of carbon distribution in the analyzed organs of transgenic lines that suggest enhanced sucrose export from leaves towards sink organs.

The tomato genome harbors four PPH-like genes

SlPPH knockdown led to diverse effects of the plant's physiology by affecting leaf senescence-associated degreening (Guyer et al. 2014), metabolism of isoprenoid-derived compounds, antioxidant capacity and carbon allocation. Nevertheless, Chl is still degraded along fruit ripening. Aiming at the identification of the missing dephytylating enzymes, a comprehensive survey for putative α/β-hydrolases homologous to SlPPH resulted in the identification of four clades in plant genomes (Fig. 5, Supplementary Table S4). One, named PPH, included the previously functionally characterized enzymes, AtPPH (Schelbert et al. 2009) and SlPPH (Guyer et al. 2014). The other three contained uncharacterized α/β-hydrolase-like genes and were named PPH-LIKE (PPHL) 1-3.

The tomato genome harbors a single copy gene in the PPH, PPHL1 and PPHL2 clade; while two paralogs were identified for the PPHL3 clade. All of the predicted protein sequences contained the PPH motif with a high degree of similarity and the conserved serine active residue (Schelbert et al 2009) suggesting that these

proteins share the catalytic domain described for SlPPH (Supplementary Fig. S4). As expression was not detected for PPHL3.1 (Solyc02g085070) in the public RNA-seq database (http://bar.utoronto.ca/efp_tomato/cgi-bin/efpWeb.cgi), this gene was not further analyzed.

The abundance of mRNA of the identified *SlPPHL* genes was profiled in leaves and along fruit ripening in wild type plants (Fig. 6 and Supplementary Table S1). The three genes showed over 5-fold more transcripts in leaves than in fruits. The mRNA amount of *SlPPHL1* decreased along ripening while *SlPPHL2* maintained constant levels from mature green towards ripe stage. Similarly to *SlPPH*, the mRNA amount of *SlPPHL3* increased at the breaker stage. It is worth pinpointing that *SlPPHLs* mRNA levels were up to 6-, 80-, 300- and 1000-fold less than *SlPPH* in leaves, mature green, breaker and ripe fruits, respectively, being *SlPPHL3* the gene with the highest expression after *SlPPH* (Supplemental Table S2). To evaluate co-silencing in *SlPPH*-knockdown plants, the *SlPPHLs* transcripts were further profiled (Fig. 7). Interestingly, a considerable level of co-silencing in leaves and fruits was verified up to 80% and 60% for *SlPPHL1* and *SlPPHL3*, respectively. *SlPPHL2* was only silenced in breaker fruits of the *SlPPH*-knockdown plants. Although the fragment of 400 bp of the hairpin RNA (RNAi) construct used for *SlPPH* silencing does not contain the conserved PPH motif, it spans a highly conserved region shared by the four genes (Supplementary Fig. S5) explaining the observed off-target silencing. The expression levels suggest that *SlPPHLs* are more likely to play a role in leaf Chl metabolism than in fruits. However, taking into account the mRNA abundance and profile fluctuation, *SlPPHL3* might also be involved in degreening during ripening, even though further experiments are needed to precisely address the role of these *SlPPHLs* genes.

Discussion

Our knowledge on Chl metabolism has significantly increased in recent years, especially regarding tetrapyrrole biosynthesis (Tanaka and Tanaka 2007), the Chl cycle (Tanaka and Tanaka 2011) and senescence-associated degradation (Hörtensteiner 2013). However, a few critical processes, such as Chl turnover (Lin et al. 2014) and ripening-induced degreening (Guyer et al. 2014) remain elusive. Interestingly, although induced upon senescence and ripening onset, *AtPPH* and *SlPPH* are transcribed in non-senescent source leaves and in developing green fruits (Schelbert et al. 2009, Lira et al. 2014). Beyond the impairment in leaf Chl degradation associated with dark-induced senescence and the delay in fruit degreening described in tomato (Guyer et al. 2014), this work investigated the effects that PPH deficiency has on the content of close metabolically-linked

compounds, photosynthetic performance and primary carbon metabolism in an integrated manner under normal growth conditions.

Although without apparent effect on vegetative growth, SlPPH deficiency led to a slight reduction in carbon assimilation. This might be a consequence of photoinhibition as evidenced by a reduced Φ_{PSII} and ETR, and by the increment in the NPQ (Table 3). The xanthophyll cycle is one of the main components of NPQ that dissipate excessively absorbed photons via harmless heat (Wilhem and Selmar 2011). In this sense, the increase in violaxanthin content observed in leaves of the *SlPPH*-knockdown plants (Table 1) is indicative of an enhancement of the xanthophyll cycle. Additionally, neoxanthin and β-carotene were also increased in leaves of transgenic plants and their role as PSII-derived singlet oxygen ($^1O_2$) quenchers has been extensively described (Pospíšil 2012). Interestingly, *SlDXS*, the first MEP enzyme encoding gene, showed upregulation while reduced level of expression of *SlLCYβ* was observed in the transgenic leaves (Fig. 3). Since no increment in Chl was verified (Supplementary Fig. S3), the alterations in the expression profile described might have resulted in higher precursor availability for carotenogenesis thus, explaining the increment in photosynthesis-associated carotenoids in *SlPPH*-knockdown plants. Interestingly, a similar transcript pattern for carotenogenesis-related genes was found in the *sgr* tomato mutant (Almeida et al. 2015a). Regarding tocopherol, the reduction of the mRNA amount of *SlVTE4* (Fig. 3) accounts for the slight decrease in α- and the increase of δ-tocopherol towards detectable levels; however, these fluctuations did not affect the total tocopherol content in transgenic plants (Table 2). These data point out that the leaves of *SlPPH*-knockdown plants accumulate carotenoids as a mechanism to attenuate photoinhibition (Fanciullino et al. 2014). Additionally, other compensatory protective mechanisms, as those that contribute to the observed increment of the hydrophilic TEAC in leaves (Fig. 2A) (*e.g.* ascorbic acid – glutathione cycle, Foyer and Shigeoka 2011), are likely to guarantee constant Fv/Fm in *SlPPH*-knockdown plants. This is in agreement with the observation in the tocopherol deficient *vte1* Arabidopsis mutant, in which, the enhancement of the non-photochemical quenching is accompanied by a compensatory increment in hydrophilic antioxidants (Kanwischer et al. 2005). Additionally, accumulation of xanthophylls was observed in response to limited PSII photoinhibition in this mutant. Furthermore, the xanthophyll and tocopherol deficient *vte1 npq1* double mutant displayed severe oxidative symptoms, pointing to the overlapping antioxidant function of both compounds (Havaux et al. 2005). Interestingly, the allocation of fixed carbon as starch diminished whereas sucrose accumulated at higher levels in leaves of the transgenic plants (Fig. 4). This shift in partitioning, away from starch and towards soluble sugars, has been described associated

to photohibition, due to the role of sucrose as stress signal and antioxidant protective agent (Bolouri-Moghaddam et al. 2010). Tomato plants showed enhanced sucrose accumulation in leaves upon low temperature treatment, together with reduction in *qP*, Φ_{PSII} and ETR, as well as increase in NPQ (Liu et al. 2012), in agreement of that observed in *SlPPH*-knockdown plants. Considering that in tomato carbon is mostly translocated in the form of sucrose (Barker et al. 2000), this carbohydrate profile hints to enhanced carbon export from leaves towards sink organs.

Accordingly, fruits of *SlPPH*-knockdown plants accumulated higher amounts of starch and soluble sugars (Fig. 4). It has already been demonstrated that the increment in sugar availability in sink organs led to the reduction of carotenoid accumulation by repressing the expression of enzyme encoding genes of the carotenoid biosynthetic pathway in tomato (Mortain-Bertrand et al. 2008) .In agreement, *SlDXS* expression is highly reduced in fruits of the *SlPPH*-deficient plants limiting the input of precursors towards GGPP. The genes encoding the first two committed steps in carotenogenesis also showed reduced levels of expression; *SlPSY1,* which is the most highly expressed paralog in fruits (The Tomato Genome Consortium, 2012) and its essential role in carotenogenesis along ripening has already been demonstrated (Fantini et al., 2013), and *SlPDS*. Thus, it is reasonable to propose that the massive reduction in carotenoid content observed in the fruits of transgenic plants (Table 1) is linked to the increased sugar availability. Additionally, the relatively higher reduction of lycopene may also be the consequence of a failure of *SlLCYβ* transcriptional repression during ripening (Fig. 3). The perturbation in Chl metabolism in *SlPPH*-knockdown plants resulted in altered tocopherol profile in fruits as well (Table 2). Taking into account that tomato mature green fruits harbor an active photosynthetic electron transport chain (Piechulla et al 1987), the slight increment in total tocopherol suggests a tuning of protective antioxidant compounds to deal with oxidative stress. Chl-degradation derived phytol is the main source of PDP for tocopherol synthesis in tomato as demonstrated by the tocopherol depletion described in *SlVTE5*-silenced plants (Almeida et al. 2015b). Although *SlVTE5* and *SlVTE6* are downregulated in *SlPPH*-knockdown fruits, such severe phenotype is not verified because of the failure of transcriptional repression of *SlGGDR* during ripening, which deflects GGPP from carotenogenesis towards PDP biosynthesis (Fig. 3) (Almeida et al. 2015a, Quadrana et al. 2013). However, the *de novo* PDP supply is not enough to maintain wild type levels of tocopherol in ripe fruits. The transgenic fruits showed TEAC inverted patterns in hydrophilic and hydrophobic fractions (Fig. 2), which negatively and positively correlated, respectively, to the variation of lipophilic antioxidant content, especially total-tocopherol. These results evidenced the existence of a compensatory regulation between

antioxidant mechanisms and reinforced the role of tocopherol as $^1O_2$ scavenger in PSII (Kaiser et al. 1990, Fukuzawa et al. 1997).

Based on the collected data and the state of knowledge, it seems reasonable to propose that PPH, beyond the already demonstrated function in senescence degreening, plays a role in photosystem-associated pigment recycling. The identification of three *SlPPH-like* genes brings new players to the Chl metabolic network for further investigation (Fig. 5). In this sense, Arabidopsis orthologs of *SlPPH-like2* and *SlPPH-like3* were previously proposed to be associated with steady-state Chl turnover (Lin et al. 2014). According to the expression pattern, *SlPPH-like3* appears as a candidate responsible for the delayed ripening-associated degreening observed in *SlPPH*-knockdown fruits (Fig. 6). It is worth pinpointing that the *SlPPHLs* co-silencing (Fig. 7) has two implications, they could partially compensate the deficiency of SlPPH in fruit degreening and also, the above described phenotypes might not only be consequence of the *SlPPH* knockdown, but also of the slight reduction in the expression of any of the *SlPPHLs*.

In summary, *SlPPH* silencing in tomato affects photosynthesis, carbon partitioning and, in an organ-specific manner, isoprenoid metabolism, which, ultimately, results in fruits with reduced levels of nutraceutical compounds but enriched levels of soluble sugars.

Materials and Methods

Plant material, growth conditions and sampling

SlPPH-silenced transgenic lines (L17, L24 and L27) were generated in a previous study (Guyer et al. 2014) by constitutively expressing an intron-spliced hairpin RNA (RNAi) construct targeted at *SlPPH* (Solyc01g088090) in *Solanum lycopersicum* (cv Ailsa Craig). T2 plants were grown in greenhouse under automatic irrigation (four times a day) in an average mean temperature of 25°C, 11.5/13 (winter/summer) light hours and 250-350 µmol m^{-2} s^{-1} of incident photo-irradiance. Plant height and leaf number were measured weekly. The sixth fully expanded leaf from the base of 7-week-old plants were harvested at the middle of the light period. Pericarp samples from fruits at mature green, breaker and ripe stages were harvested approximately at 39 (displaying jelly placenta), 42 and 52 days after anthesis, respectively. All samples were frozen in liquid N_2, powdered and

stored at -80°C. For tocopherol content determination, leaf and pericarp samples were dried by lyophilization before extraction.

qPCR analysis

RNA extraction, complementary DNA (cDNA) synthesis, primer design and qPCR assays were performed as described by Quadrana et al. (2013). Primer sequences used are detailed in Supplementary Table S3. qPCR reactions were carried out in a 7500 real-time PCR system (Applied Biosystems) using 2X SYBR Green Master Mix reagent (Life Technologies) in a 20 µL final volume. Absolute fluorescence data were analyzed using the LinRegPCR software package (Ruijter et al. 2009) in order to obtain quantitation cycle (Cq) values and calculate PCR efficiency. Expression values were normalized against the geometric mean of two reference genes, TIP41 and EXPRESSED, according to Quadrana et al. (2013). A permutation test lacking sample distribution assumptions (Pfaffl et al. 2002) was applied to detect statistical differences ($P < 0.05$) in expression ratios using the algorithms in the fgStatistics software package version 17/05/2012 (Di Rienzo 2009).

Tocopherol and pigment quantification

Tocopherols were extracted from approximately 25 mg dry weight as described in Almeida et al. (2015a). The samples were adjusted to 4 mL final volume. Aliquots of 3 mL were dried under N_2 and dissolved in 200 µL of mobile phase composed of hexane/*tert*-butyl methyl ether (90:10). Chromatography was carried out on a Hewlett–Packard series 1100 HPLC system coupled with a fluorescence detector (Agilent Technologies series 1200) on a normal-phase column (LiChrosphere® 100 Diol Si; 250 mm x 4.0 mm, 5 µm; Agilent Technologies, Germany) at room temperature, with the mobile phase running isocratically at 1 mL min^{-1}. Eluted compounds were detected by excitation at 295 nm and fluorescence was quantified at 330 nm.

Chlorophyll extraction was carried out as described in Porra et al. (1989). One mL of dimethylformamide (DMF) was added to 100 mg or 300 mg of fresh weight for leaf or fruit samples, respectively. After sonication for five min and further centrifugation of 9000 g for 10 min, the supernatant was collected. The procedure was repeated until total removal of tissue green colour. Spectrophotometer measurements were performed at 664 and 647 nm.

Carotenoid extraction was modified from Sérino et al. (2009). Aliquots of 200 mg of fresh weight were sequentially extracted with a solution of saturated NaCl, dichloromethane and hexane:diethyl ether (1:1). After centrifugation, the supernatant was collected and the last step was repeated three more times. Samples were dried by vacuum and dissolved in 200 µL of acetonitrile. Chromatography was carried out on Agilent Technologies series 1100 HPLC system on a normal-phase column Phenomenex (Luna C18; 250 x 4.6 mm; 5 µm particle diameter) at room temperature with a flow rate of 1 mL min^{-1}. The mobile phase was a gradient of ethyl acetate (A) and acetonitrile:water 9:1 (B): 0-4 min with 20% A/80% B; 4-30 min with 65% A/35% B; 30-35 min with 65% A/35% B; 35-40 min with 20% A/80% B. Eluted compounds were detected between 340-700 nm and quantified at 450 nm.

Trolox equivalent antioxidant capacity (TEAC)

Leaf and pericarp samples of 100 and 500 mg fresh weight, respectively, were ground in liquid nitrogen and subsequently homogenized in 1 mL of 100 mM sodium acetate buffer pH 7.0. The homogenate was incubated at 4°C for 30 min and then centrifuged for 10 min at 4°C at 5000 *g*. The supernatant was immediately analyzed for hydrophilic antioxidant activity and the pellet was resuspended in 1.5 mL hexane, incubated at 4°C for 30 min and then centrifuged for 10 min at 4°C at 5000 *g*. This procedure was performed three times and the organic extract was reduced to 500 µL under vacuum and immediately analyzed for lipophilic antioxidant activity. Both hydrophilic and lipophilic antioxidant activities were specrophotometrically determined as the deactivation of an activated 2,2'-azino-bis(3-ethylbenzothiazoline-6-sulfonic acid ($ABTS^{+\bullet}$) solution prepared as described in Re et al. (1999) and compared to a standard curve of 6-hydroxy-2,5,7,8-tetramethylchroman-2-carboxylic acid (Trolox). Absorbance was read at 734 nm after 2 h of incubation at 25°C and the results were expressed as Trolox Equivalent Antioxidant Capacity (TEAC).

Leaf gas exchange and fluorescence measurements

Gas exchange and chlorophyll fluorescence parameters were measured in the sixth fully expanded leaf from the base of 7-week-old plants between 10 and 12 h using a portable open gas-exchange system incorporating infra-red CO_2 and water vapor analysers (LI-6400XT system; LI-COR) equipped with an integrated modulated

chlorophyll fluorometer (LI-6400-40; LI-COR). Reference CO_2 concentration was held at 400 µmol mol^{-1} and leaf temperature at 28˚C for all measurements. Air humidity inside the leaf chamber was equivalent to values measured inside the greenhouse (approximately 75%). Carbon assimilation rate (*A*), leaf stomatal conductance (g_s), leaf dark respiration (R_d), transpiration (*E*) and fluorescence parameters were measured at 800 µmol PPFD m^{-2} s^{-1}. For the values of minimal (*Fo*) and maximal (*Fm*) fluorescence and leaf dark respiration, leaves were dark-adapted for 30 min before a saturating pulse of light. The parameters derived from chlorophyll fluorescence, including dark-adapted PSII maximum quantum efficiency (*Fv/Fm*), proportion of open PSII centers (photochemical quenching, *qP*), PSII operating efficiency (Φ_{PSII}), non-photochemical quenching (NPQ) and electron transport rate (ETR) were calculated according to Maxwell and Johnson (2000).

Starch and soluble sugars quantification

Soluble sugars and starch extraction and quantification were performed as described in Freschi et al. (2010) with some modifications. Briefly, 100 and 300 mg of fresh weight of leaf and pericarp samples, respectively, were extracted in 1 mL 80% ethanol for 15 min at 80°C and the supernatants were recovered by centrifugation (5000 *g*, 15 min). Pellets were re-extracted five times and all supernatants were combined and reduced to dryness under vacuum. Starch content was determined from dried pellets as described in Suguiyama et al. (2014). The supernatant residue was resuspended in 50 µL pyridine and derivatized for 40 min at 60°C with 20 µL of N,O-bis(trimethylsilyl)trifluoroacetamide with 1% of trimethylchlorosilane. Sample volumes of 1 µL of the trimethylsilylated extracts were analyzed on a gas chromatograph coupled to a mass spectrometer (model GCMS-QP2010 SE, Shimadzu) and total ion current spectra were recorded in the mass range of 50–700 atomic mass units in scanning mode. The chromatograph was equipped with a fused-silica capillary column (30 m, ID 0.25 mm, 0.50 µm thick internal film) DB-5 MS stationary phase using helium as the carrier gas at a flow rate of 4.5 mL min^{-1}. The initial running condition was 100°C for 5 min, followed by a gradient up to 320°C at 8°C min^{-1}. The injector temperature was 250°C and the following MS operating parameters were used: ionization voltage, 70 eV (electron impact ionization); ion source temperature, 230°C; interface temperature, 260°C. The endogenous metabolite concentration was obtained by comparing the peak areas of the chromatograms with commercial standards.

Phenetic analysis

For the phenetic analysis, Phytozome v10.1 database (Goodstein et al. 2012) was surveyed for AtPPH homologous sequences (Supplementary Table S4). The retrieved protein sequences were aligned by Clustal in MEGA 6.0 software (Tamura et al. 2013) using default parameters. The tree reconstruction from the obtained alignment was performed using PHYML 3.0 algorithm (Guindon et al. 2010) hosted at http://www.hiv.lanl.gov/content/sequence/PHYML/interface.html with the following parameters: LG substitution model, four substitutions rate categories, tree optimization by topology and branch length and, improvement by subtree pruning and regrafting. From the dataset the proportion of invariable sites, equilibrium of frequencies and gamma shape parameter were estimated. Branches were supported by SH-like support.

Data analyses

Differences in parameters were analyzed in Infostat software version 17/06/2015 (Di Rienzo et al. 2011). When the data set showed homoscedasticity, *t*-test ($P<0.05$) was performed to compare transgenic lines against wild type control genotype. In the absence of homoscedasticity, a non-parametric comparison was performed by applying Mann-Whitney. test ($P<0.05$). All values represent the mean of at least three biological replicates. A parameter was considered to be affected by *SlPPH* silencing if at least two out of the three transgenic lines differed significantly from the wild type genotype.

Funding

BSL, DR, JA and APS were recipients of FAPESP fellowships and, MR and MB were funded by a fellowship from CNPq. This work was partially supported by grants from FAPESP (Brazil), CNPq (Brazil) and USP (Brazil). SH is supported by grants from the Swiss National Science Foundation.

Disclosures

The authors have no conflicts of interest to declare.

References

Almeida, J., Quadrana, L., Asís, R., Setta, N., de Godoy, F., Bermúdez, L., et al. (2011) Genetic dissection of vitamin E biosynthesis in tomato. *J. Exp. Bot*. 62(11): 3781-3798.

Almeida, J., Asís, R., Molineri, V.N., Sestari, I., Lira, B.S., Carrari, F., et al. (2015a) Fruits from ripening impaired, chlorophyll degraded and jasmonate insensitive tomato mutants have altered tocopherol content and composition. *Phytochem*. 111: 72-83.

Almeida, J., Azevedo, M.S., Spicher, L., Glauser,. G, vom Dorp, K., Guyer, L., et al. (2015b). Down-regulation of tomato PHYTOL KINASE strongly impairs tocopherol biosynthesis and affects prenyllipid metabolism in an organ-specific manner. *J. Exp. Bot.* doi: 10.1093/jxb/erv504.

Barker, L., Kühn, C., Weise, A., Schulz, A., Gebhardt, C., Hirner, B., et al. (2000) SUT2, a putative sucrose sensor in sieve elements. *The Plant Cell.* 12(7): 1153-1164.

Barsan, C., Zouine, M., Maza, E., Bian, W., Egea, I., Rossignol, M., et al. (2012) Proteomic analysis of chloroplast-to-chromoplast transition in tomato reveals metabolic shifts coupled with disrupted thylakoid biogenesis machinery and elevated energy-production components. *Plant Physiol.* 160(2): 708-725.

Bolouri-Moghaddam, M.R., Le Roy, K., Xiang, L., Rolland, F., and Van den Ende, W. (2010). Sugar signalling and antioxidant network connections in plant cells. *FEBS journal*. 277(9): 2022-2037.

Canene-Adams, K., Campbell, J.K., Zaripheh, S., Jeffery, E.H. and Erdman, J.W. (2005) The tomato as a functional food. *The Journal of Nutrition*. 135(5): 1226-1230.

Chun, J., Lee, J., Ye, L., Exler, J. and Eitenmiller, R.R. (2006) Tocopherol and tocotrienol contents of raw and processed fruits and vegetables in the United States diet. *J Food Compos Anal.* 19(2): 196-204.

DellaPenna, D. and Pogson, B. J. (2006) Vitamin synthesis in plants: tocopherols and carotenoids. *Annu. Rev. Plant Biol.* 57: 711-738.

Di Rienzo, J.A. (2009) Statistical software for the analysis of experiments of functional genomics. RDNDA, Argentina.

493 Di Rienzo, J.A., Casanoves, F., Balzarini, M.G., Gonzalez, L., Tablada, M. and Robledo, Y.C. (2011) InfoStat
494 versión 2011. Grupo InfoStat, FCA, Universidad Nacional de Córdoba, Argentina. *URL http://www.*
495 *infostat. com. ar.*
496 Egea, I., Bian, W., Barsan, C., Jauneau, A., Pech, J.C., Latché, A., et al. (2011) Chloroplast to chromoplast
497 transition in tomato fruit: spectral confocal microscopy analyses of carotenoids and chlorophylls in
498 isolated plastids and time-lapse recording on intact live tissue. *Ann. Bot-London.* 108(2): 291-297.
499 Fanciullino, A.L., Bidel, L.P.R., and Urban, L. (2014). Carotenoid responses to environmental stimuli: integrating
500 redox and carbon controls into a fruit model. *Plant Cell Environ.*. 37(2): 273-289.
501 Fantini, E., Falcone, G., Frusciante, S., Giliberto, L., Giuliano, G. (2013) Dissection of tomato lycopene
502 biosynthesis through virus-induced gene silencing. *Plant Physiol*. 163: 986–998.
503 Foyer, C.H. and Shigeoka, S. (2011) Understanding oxidative stress and antioxidant functions to enhance
504 photosynthesis. *Plant Physiol.* 155(1): 93-100.
505 Freschi, L., Rodrigues, M.A., Tine, M.A. and Mercier, H. (2010) Correlation between citric acid and nitrate
506 metabolisms during CAM cycle in the atmospheric bromeliad *Tillandsia pohliana*. *J. Plant Physiol*. 167:
507 1577-1583.
508 Fukuzawa, K., Matsuura, K., Tokumura, A., Suzuki, A. and Terao, J. (1997) Kinetics and dynamics of singlet
509 oxygen scavenging by alpha-tocopherol in phospholipid model membranes. *Free Radical Bio. Med*. 22:
510 923-930.
511 Goodstein, D.M., Shu, S., Howson, R., Neupane, R., Hayes, R.D., Fazo, J., et al. (2012) Phytozome: a comparative
512 platform for green plant genomics. *Nucleic Acids Res*. 40(D1): D1178-D1186.
513 Guindon, S., Dufayard, J.F., Lefort, V., Anisimova, M., Hordijk, W. and Gascuel, O. (2010) New algorithms and
514 methods to estimate maximum-likelihood phylogenies: assessing the performance of PhyML 3.0. *Syst*
515 *Biol*. 59(3): 307-321.
516 Guyer, L., Schelbert-Hofstetter, S., Christ, B., Lira, B.S., Rossi, M. and Hörtensteiner, S. (2014) Different
517 mechanisms are responsible for chlorophyll dephytylation during fruit ripening and leaf senescence in
518 tomato. *Plant Physiol*. 166: 44-56.
519 Havaux, M., Eymery, F., Porfirova, S., Rey, P. and Dörmann, P. (2005) Vitamin E protects against photoinhibition
520 and photooxidative stress in *Arabidopsis thaliana*. *The Plant Cell*. 17(12): 3451-3469.
521 Hörtensteiner, S. (2013) Update on the biochemistry of chlorophyll breakdown. *Plant Mol Biol*. 82: 505-517.

Ischebeck, T., Zbierzak, A.M., Kanwischer, M. and Dörmann, P. (2006) A salvage pathway for phytol metabolism in Arabidopsis. *J. Biol. Chem*. 281(5): 2470-2477.

Jahns, P. and Holzwarth, A.R. (2012) The role of the xanthophyll cycle and of lutein in photoprotection of photosystem II. *BBA-Bioenergetics.* 1817(1): 182-193.

Kaiser, S., Di Mascio, P., Murphy, M.E. and Sies, H. (1990) Physical and chemical scavenging of singlet molecular oxygen by tocopherols. *Arch. Biochem. Biophys.* 277: 101-108.

Kanwischer, M., Porfirova, S., Bergmüller, E. and Dörmann, P. (2005) Alterations in tocopherol cyclase activity in transgenic and mutant plants of Arabidopsis affect tocopherol content, tocopherol composition, and oxidative stress. *Plant Physiol*. 137(2): 713-723.

Lin, Y.P., Lee, T.Y., Tanaka, A. and Charng, Y.Y. (2014) Analysis of an Arabidopsis heat-sensitive mutant reveals that chlorophyll synthase is involved in reutilization of chlorophyllide during chlorophyll turnover. *The Plant J*. 80(1): 14-26.

Lira, B.S., de Setta, N., Rosado, D., Almeida, J., Freschi, L. and Rossi, M. (2014) Plant degreening: evolution and expression of tomato (*Solanum lycopersicum*) dephytylation enzymes. *Gene*. 546(2): 359-366.

Liu, Y.F., Qi, M.F. and Li, T.L. (2012) Photosynthesis, photoinhibition, and antioxidant system in tomato leaves stressed by low night temperature and their subsequent recovery. *Plant Sci*. 196: 8-17.

Luo, Z., Zhang, J., Li, J., Yang, C., Wang, T., Ouyang, B., et al. (2013) A STAY-GREEN protein SlSGR1 regulates lycopene and β-carotene accumulation by interacting directly with SlPSY1 during ripening processes in tomato. *New Phytol*. 198(2): 442-452.

Maxwell, K. and Johnson, G.N. (2000) Chlorophyll fluorescence - a practical guide. *J Exp Bot.* 51(345): 659-668.

Mortain-Bertrand, A., Stammitti, L., Telef, N., Colardelle, P., Brouquisse, R., Rolin, D., and Gallusci, P. (2008). Effects of exogenous glucose on carotenoid accumulation in tomato leaves. *Physiol Plant*. 134(2): 246-256.

Pfaffl, M.W., Horgan, G.W. and Dempfle, L. (2002) Relative expression software tool (REST©) for group-wise comparison and statistical analysis of relative expression results in real-time PCR. *Nucleic Acids Res*. 30(9): e36-e36.

Piechulla, B., Glick, R.E., Bahl, H., Melis, A. and Gruissem, W. (1987) Changes in photosynthetic capacity and photosynthetic protein pattern during tomato fruit ripening. *Plant Physiol.* 84(3): 911-917.

Porra, R.J., Thompson, W.A. and Kriedemann, P.E. (1989) Determination of accurate extinction coefficients and simultaneous equations for assaying chlorophylls a and b extracted with four different solvents: verification of the concentration of chlorophyll standards by atomic absorption spectroscopy. *BBA-Bioenergetics.* 975(3): 384-394.

Pospíšil, P. (2012) Molecular mechanisms of production and scavenging of reactive oxygen species by photosystem II. *BBA-Bioenergetics*. 1817(1): 218-231.

Quadrana, L., Almeida, J., Otaiza, S. N., Duffy, T., Da Silva, J.V.C., de Godoy, F., et al (2013) Transcriptional regulation of tocopherol biosynthesis in tomato. *Plant Mol. Biol*. 81(3): 309-325.

Re, R., Pellegrini, N., Proteggente, A., Pannala, A., Yang, M. and Rice-Evans, C. (1999) Antioxidant activity applying an improved ABTS radical cation decolorization assay. *Free Radical Bio. Med.* 26: 1231-1237.

Rossi, M., Bermudez, L. and Carrari, F. (2015) Crop yield: challenges from a metabolic perspective. *Curr. Opin. Plant Biol*. 25: 79-89.

Ruijter, J.M., Ramakers, C., Hoogaars, W.M.H., Karlen, Y., Bakker, O., Van den Hoff, M.J.B. and Moorman, A.F.M. (2009) Amplification efficiency: linking baseline and bias in the analysis of quantitative PCR data. *Nucleic Acids Res*. 37(6): e45-e45.

Sakuraba, Y., Schelbert, S., Park, S.Y., Han, S.H., Lee, B. D., Andrès, C. B., et al. (2012) STAY-GREEN and chlorophyll catabolic enzymes interact at light-harvesting complex II for chlorophyll detoxification during leaf senescence in Arabidopsis. *The Plant Cell.* 24(2): 507-518.

Sakuraba, Y., Park, S.Y., Kim, Y.S., Wang, S.H., Yoo, S.C., Hörtensteiner, S., and Paek, N.C. (2014). Arabidopsis STAY-GREEN2 is a negative regulator of chlorophyll degradation during leaf senescence. *Mol. Plant*. 7(8): 1288-1302.

Schelbert, S., Aubry, S., Burla, B., Agne, B., Kessler, F., Krupinska, K. and Hörtensteiner, S. (2009) Pheophytin pheophorbide hydrolase (pheophytinase) is involved in chlorophyll breakdown during leaf senescence in Arabidopsis. *The Plant Cell.* 21(3): 767-785.

Sérino, S., Gomez, L., Costagliola, G.U.Y. and Gautier, H. (2009) HPLC assay of tomato carotenoids: validation of a rapid microextraction technique. *J. Agr. Food Chem*. 57(19): 8753-8760.

Seymour, G.B., Chapman, N.H., Chew, B.L. and Rose, J.K. (2013). Regulation of ripening and opportunities for control in tomato and other fruits. *Plant Biotechnol. J.* 11(3): 269-278.

578 Suguiyama, V.F., Silva, E.A., Meirelles, S.T., Centeno, D.C. and Braga, M.R. (2014) Leaf metabolite profile of the
579 Brazilian resurrection plant *Barbacenia purpurea* Hook. (Velloziaceae) shows two time-dependent
580 responses during desiccation and recovering. *Front. Plant Sci*. 5: 96.
581 Tamura, K., Stecher, G., Peterson, D., Filipski, A. and Kumar, S. (2013) MEGA6: molecular evolutionary genetics
582 analysis version 6.0. *Mol. Biol. Evol*. 30(12): 2725-2729.
583 Tanaka, R. and Tanaka, A. (2007) Tetrapyrrole biosynthesis in higher plants. *Annu Rev Plant Biol*. 58: 321-346.
584 Tanaka, R. and Tanaka, A. (2011) Chlorophyll cycle regulates the construction and destruction of the light-
585 harvesting complexes. *BBA-Bioenergetics.* 1807(8): 968-976.
586 The Tomato Genome Consortium. (2012) The tomato genome sequence provides insights into fleshy fruit
587 evolution. *Nature* 485: 635–641.
588 Thomas, H. and Howarth, C.J. (2000) Five ways to stay green. *J. Exp. Bot.* 51, 329-337.
589 Thomas, H. and Ougham, H. (2014) The stay-green trait. *J. Exp. Bot*. 65(14), 3889-3900.
590 Valentin, H.E., Lincoln, K., Moshiri, F., Jensen, P.K., Qi, Q., Venkatesh, T. V., et al. (2006) The Arabidopsis vitamin
591 E pathway gene5-1 mutant reveals a critical role for phytol kinase in seed tocopherol biosynthesis. *The*
592 *Plant Cell*. 18(1): 212-224.
593 Vass, I. and Cser, K. (2009) Janus-faced charge recombinations in photosystem II photoinhibition. *Trends in*
594 *Plant Sci.* 14(4): 200-205.
595 vom Dorp, K., Hölzl, G., Plohmann, C., Eisenhut, M., Abraham, M., Weber, A.P., et al. (2015) Remobilization of
596 Phytol from Chlorophyll Degradation Is Essential for Tocopherol Synthesis and Growth of Arabidopsis.
597 *The Plant Cell*. doi: 10.1105/tpc.15.00395.
598 Wilhelm, C. and Selmar, D. (2011) Energy dissipation is an essential mechanism to sustain the viability of plants:
599 the physiological limits of improved photosynthesis. *J. Plant Physiol.* 168(2): 79-87.
600 Zhang, W., Liu, T., Ren, G., Hörtensteiner, S., Zhou, Y., Cahoon, E.B. and Zhang, C. (2014) Chlorophyll
601 degradation: the tocopherol biosynthesis-related phytol hydrolase in Arabidopsis seeds is still missing.
602 *Plant Physiol*. 166(1): 70-79.
603 Zhang, C., Zhang, W., Ren, G., Li, D., Cahoon, R.E., Chen, M., et al (2015) Chlorophyll synthase under epigenetic
604 surveillance is critical for vitamin E synthesis and altered expression impacts tocopherol levels in
605 Arabidopsis. *Plant Physiol*. 168(4): 1503-1511.
606

Figure Legends

Fig. 1 Chlorophyll, tocopherol and carotenoid metabolism. Schematic representation of the interconnection between chlorophyll synthesis and degradation (green), carotenogenesis (orange) and tocopherol biosynthetic (blue) pathways. Dotted lines represent that intermediary steps were omitted. Enzymes whose genes have transcriptionally been profiled in this work are indicated. Enzymes and compounds are named according to the following abbreviations: DXS, 1-deoxy-d-xylulose-5-P synthase; GGDR, geranylgeranyl diphosphate reductase; PSY, phytoene synthase; PDS, phytoene desaturase; LCYβ, chloroplast-specific β-lycopene cyclase; CYCβ, chromoplast-specific β-lycopene cyclase; GGPP, geranylgeranyl diphosphate; PDP, phytyl diphosphate; PP, phytyl phosphate; PPH, pheophytinase; PAO, pheophorbide a oxygenase; pFCC, primary fluorescent chlorophyll catabolite; VTE5, phytol kinase; VTE6, phytyl phosphate kinase; MPBQ, 2-methyl-6-geranylgeranylbenzoquinol; VTE1, tocopherol cyclase; VTE2, homogentisate phytyl transferase; VTE3, 2,3-dimethyl-5-phytylquinol methyltransferase; VTE4, tocopherol C-methyl transferase; MEP: methylerythritol 4-phosphate pathway. Adapted from Almeida et al. (2015b).

Fig. 2 Trolox equivalent antioxidant capacity (TEAC) in *SlPPH*-knockdown lines. The TEAC assay was addressed in hydrophilic (A) and lipophilic (B) extracts of leaves and fruits at mature green and ripe stages. Values represent the mean ± SD from at least three biological replicates. Statistically significant differences ($P<0.05$) between the control genotype and transgenic lines are marked with an asterisk.

Fig. 3 Transcript profile of chlorophyll degradation, carotenogenesis and tocopherol biosynthetic genes in leaves and along fruit ripening of *SlPPH*-knockdown lines. Heatmap representation of the statistically significant ($P<0.05$) relative transcript amount compared to the corresponding wild type sample. The expression values are detailed in Supplementary Table S1. The abbreviations indicate: *SlSGR*, stay-green*; SlPAO*, pheophorbide *a* oxygenase; *SlDXS*, 1-deoxy-d-xylulose-5-P synthase; *SlGGDR*, geranylgeranyl diphosphate reductase; *SlVTE1*, tocopherol cyclase; *SlVTE2*, homogentisate phytyl transferase; *SlVTE3*, 2,3-dimethyl-5-phytylquinol methyltransferase; *SlVTE4*, tocopherol C-methyl transferase; *SlVTE5*, phytol kinase; *SlVTE6*, phytyl phosphate kinase; *SlPSY*, phytoene synthase; *SlPDS*, phytoene desaturase; *SlLCYβ*, chloroplast-specific β-lycopene cyclase; *SlCYCβ*, chromoplast-specific β-lycopene cyclase; LF, leaf; MG, mature green fruit pericarp; BR, breaker fruit

pericarp; RR, ripe fruit pericarp. Values represent means from at least three biological replicates. *SlVTE3(2)* was not evaluated in fruits (grey boxes) because it is leaf-specific (Quadrana et al. 2013).

Fig. 4 Starch and soluble sugar content in *SlPPH*-knockdown lines. The content of starch and soluble sugars (glucose, fructose and sucrose) was measured in leaves and fruits at the mature green and ripe stages. Values represent the mean ± SD from at least three biological replicates. Statistically significant differences (P<0.05) between the control genotype and transgenic lines are marked with an asterisk.

Fig. 5 Phenetic analysis of PPH homologous protein sequences. PPH homologs were identified in the Phytozome database (Supplementary Tables S4). Tree topology reveals four clades: the already functionally characterized PPH clade and three still uncharacterized clades that were named PPH-LIKE1-3.

Fig. 6 Transcript profile of *SlPPH* and *SlPPHLs* genes in leaves and along fruit ripening of the wild type genotype. Data represent the mean ± SD from at least three biological replicates and are expressed as relative transcript amount compared to the corresponding mature green stage. Statistically significant differences (P<0.05) compared to the mature green stage are marked with an asterisk.

Fig. 7 Transcript profile of *SlPPHLs* in *SlPPH*-knockdown plants in leaves and along fruit ripening. Data represent the mean ± SD from at least three biological replicates and are expressed as relative transcript amount compared to the corresponding wild type sample. Statistically significant differences (P<0.05) compared to the mature green stage are marked with an asterisk.

Supplementary data

Supplementary Fig. S1 *SlPPH* transcript profile in *SlPPH*-knockdown lines.

Supplementary Fig. S2 Vegetative growth of *SlPPH*-knockdown lines.

Supplementary Fig. S3 Chlorophyll content and impairment of age-induced senescence-associated degreening in *SlPPH*-knockdown lines.

Supplementary Fig. S4 Protein sequence alignment of AtPPH, SlPPH and SlPPHLs.

Supplementary Fig. S5 Alignment of *SlPPHLs* along the fragment of the hairpin RNA (RNAi) construct used for *SlPPH*-knockdown plants.

Supplementary Table S1. Expression values of chlorophyll degradation, carotenogenesis and tocopherol biosynthetic genes in leaves and along fruit ripening of *SlPPH*-knockdown lines.

Supplementary Table S2. Relative transcript ratio of *SlPPH* and *SlPPHL*s.

Supplementary Table S3. Primers used for qPCR.

Supplementary Table S4. Sequences used for alignment.

673 **Table 1. Carotenoid contents in *SlPPH* knockdown lines.**

	WT	L17	L24	L27
Leaf				
Neoxanthin	41.82 ± 7.63	**52.39 ± 6.92**	**65.56 ± 8.8**	**56.11 ± 6.97**
Violaxanthin	36.57 ± 10.36	**66.23 ± 10.17**	**71.36 ± 12.65**	**70.87 ± 14.32**
Lutein	52.75 ± 7.05	53.03 ± 7.38	61.25 ± 6.37	59.94 ± 4.69
Lycopene	ND	ND	ND	ND
β-Carotene	39.16 ± 6.08	**60.81 ± 5.66**	**64.32 ± 6.4**	**69.7 ± 10.5**
Mature green fruit				
Neoxanthin	2.00 ± 0.39	1.81 ± 0.24	2.28 ± 0.18	2.22 ± 0.6
Violaxanthin	2.16 ± 0.32	**1.80 ± 0.12**	2.38 ± 0.23	2.33 ± 0.5
Lutein	6.16 ± 0.99	5.74 ± 0.69	6.22 ± 0.52	5.76 ± 1.32
Lycopene	ND	ND	ND	ND
β-Carotene	1.74 ± 0.10	1.77 ± 0.16	**2.07 ± 0.15**	1.89 ± 0.07
Ripe fruit				
Neoxanthin	0.19 ± 0.02	**0.14 ± 0.01**	**0.13 ± 0.01**	**0.14 ± 0.02**
Violaxanthin	0.50 ± 0.05	**0.38 ± 0.02**	**0.34 ± 0.06**	**0.38 ± 0.04**
Lutein	2.40 ± 0.22	2.20 ± 0.11	2.24 ± 0.13	2.22 ± 0.16
Lycopene	411.04 ± 11.51	**326.42 ± 34.76**	**271.3 ± 16.62**	**283.32 ± 10.53**
β-Carotene	10.13 ± 0.72	**9.02 ± 0.32**	**7.25 ± 0.78**	**7.88 ± 1.28**

674 Statistically significant differences between the wild type (WT) control and transgenic lines are indicated in
675 bold terms (*t*-test, $P<0.05$). Values represent means ± SD from at least three biological replicates. Values
676 are expressed in μg/g fresh weight. ND: Not Detected.
677

678 **Table 2. Tocopherol content in *SlPPH*-knockdown lines.**

	WT	L17	L24	L27
Leaf				
α-tocopherol	326.49 ± 3.59	322.41 ± 12.32	**301.85 ± 13.54**	308.35 ± 15.61
β-tocopherol	ND	ND	ND	ND
ϒ-tocopherol	5.01 ± 0.94	6.11 ± 0.88	6.32 ± 1.04	4.36 ± 0.48
δ-tocopherol	ND	**2.05 ± 0.33**	**2.31 ± 0.19**	**1.81 ± 0.20**
Total-tocopherol	331.50 ± 6.07	330.57 ± 22.65	310.48 ± 14.42	314.51 ± 20.09
Mature green fruit				
α-tocopherol	134.88 ± 1.97	**149.08 ± 8.38**	**141.04 ± 2.81**	**146.74 ± 4.90**
β-tocopherol	2.78 ± 0.18	2.38 ± 0.22	2.60 ± 0.36	2.70 ± 0.22
ϒ-tocopherol	6.28 ± 0.79	**11.86 ± 0.50**	**13.96 ± 2.01**	**14.33 ± 1.53**
δ-tocopherol	ND	ND	ND	ND
Total-tocopherol	143.94 ± 2.43	**163.32 ± 4.32**	**157.60 ± 3.58**	**163.77 ± 2.77**
Ripe fruit				
α-tocopherol	145.54 ± 17.48	**167.40 ± 13.76**	**165.67 ± 22.62**	**170.72 ± 30.55**
β-tocopherol	3.24 ± 0.18	2.85 ± 0.27	3.22 ± 0.13	3.00 ± 0.21
ϒ-tocopherol	93.07 ± 8.23	**27.47 ± 6.11**	**36.49 ± 3.42**	**50.21 ± 4.39**
δ-tocopherol	2.10 ± 0.15	**1.28 ± 0.08**	**1.35 ± 0.10**	**1.31 ± 0.11**
Total-tocopherol	243.94 ± 25.88	**198.99 ± 25.41**	**206.72 ± 11.56**	**225.23 ± 17.69**

679 Statistically significant differences between the wild type (WT) control and transgenic lines are indicated in bold
680 terms (*t*-test, $P<0.05$). Values represent means ± SD from at least three biological replicates. Values are expressed in
681 μg/g dry weight. ND: Not Detected.
682

683 **Table 3. Photosynthetic parameters in *SlPPH*-knockdown lines.**

	WT	L17	L24	L27
A	13.35 ± 0.86	**12.16 ± 0.89**	**11.92 ± 0.93**	**11.85 ± 0.94**
R_d	2.46 ± 0.17	2.31 ± 0.14	2.37 ± 0.20	2.42 ± 0.17
E	4.05 ± 0.17	3.92 ± 0.28	3.90 ± 0.14	4.03 ± 0.14
g_s^2	0.34 ± 0.02	0.30 ± 0.04	0.31 ± 0.03	0.31 ± 0.04
Fv/Fm	0.61 ± 0.02	0.62 ± 0.02	0.63 ± 0.02	0.60± 0.01
qP	0.38 ± 0.01	**0.33 ± 0.03**	**0.34 ± 0.03**	**0.32 ± 0.03**
NPQ	0.97 ± 0.04	1.01 ± 0.05	**1.18 ± 0.12**	**1.15 ± 0.07**
Φ_{PSII}	0.22 ± 0.01	**0.18 ± 0.01**	**0.19 ± 0.01**	**0.20 ± 0.01**
ETR	98.45 ± 3.11	**84.98 ± 2.99**	**86.51 ± 7.49**	**85.27 ± 8.71**

684 Photosynthetic parameters were measured in the sixth fully expanded leaf from the base of
685 7-week-old plants. Statistically significant differences between the wild type (WT) control and
686 transgenic lines are indicated in bold terms (*t*-test, $P<0.05$). Values represent means ± SD
687 from at least three biological replicates. Carbon assimilation rate (*A*) and leaf dark respiration
688 (R_d) are expressed in µmol $CO_2.m^{-2}.s^{-1}$. Transpiration (*E*) and leaf stomatal conductance (g_s)
689 are expressed in mol $H_2O.m^{-2}.s^{-1}$. *Fv/Fm*: dark-adapted PSII maximum quantum efficiency. *qP:*
690 proportion of open PSII centers. Φ_{PSII}: PSII operating efficiency. NPQ: non-photochemical
691 quenching. ETR: electron transport rate.
692

Figure 1

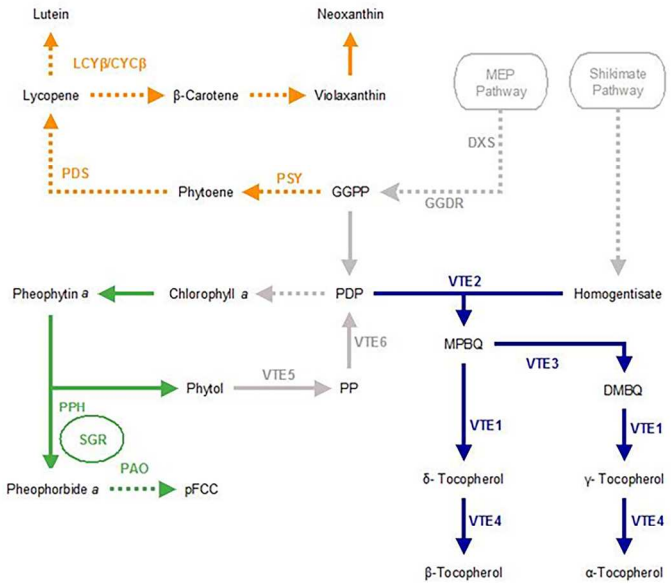

Fig. 1 Chlorophyll, tocopherol and carotenoid metabolism. Schematic representation of the interconnection between chlorophyll synthesis and degradation (green), carotenogenesis (orange) and tocopherol biosynthetic (blue) pathways. Dotted lines represent that intermediary steps were omitted. Enzymes whose genes have transcriptionally been profiled in this work are indicated. Enzymes and compounds are named according to the following abbreviations: DXS, 1-deoxy-d-xylulose-5-P synthase; GGDR, geranylgeranyl diphosphate reductase; PSY, phytoene synthase; PDS, phytoene desaturase; LCYβ, chloroplast-specific β-lycopene cyclase; CYCβ, chromoplast-specific β-lycopene cyclase; GGPP, geranylgeranyl diphosphate; PDP, phytyl diphosphate; PP, phytyl phosphate; PPH, pheophytinase; PAO, pheophorbide a oxygenase; pFCC, primary fluorescent chlorophyll catabolite; VTE5, phytol kinase; VTE6, phytyl phosphate kinase; MPBQ, 2-methyl-6-geranylgeranylbenzoquinol; VTE1, tocopherol cyclase; VTE2, homogentisate phytyl transferase; VTE3, 2,3-dimethyl-5-phytylquinol methyltransferase; VTE4, tocopherol C-methyl transferase; MEP: methylerythritol 4-phosphate pathway. Adapted from Almeida et al. (2015b).
209x303mm (300 x 300 DPI)

Figure 2

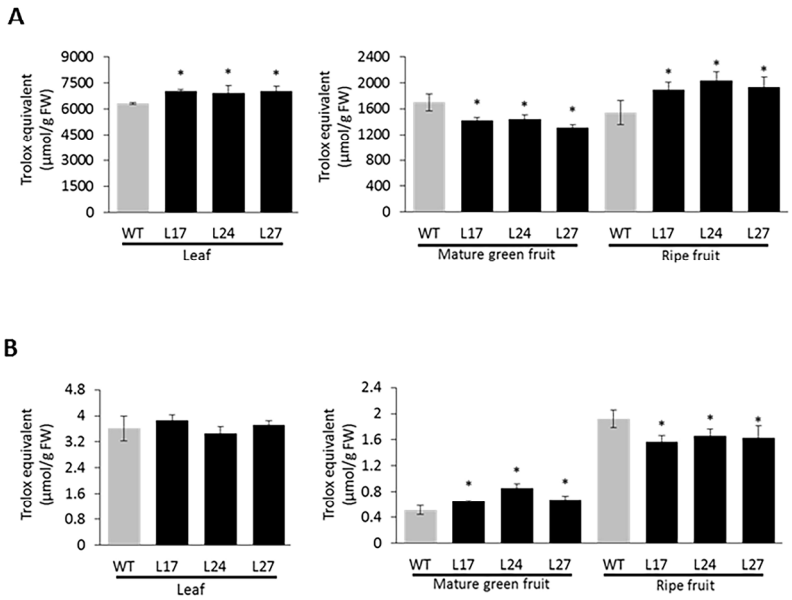

Fig. 2 Trolox equivalent antioxidant capacity (TEAC) in SlPPH-knockdown lines. The TEAC assay was addressed in hydrophilic (A) and lipophilic (B) extracts of leaves and fruits at mature green and ripe stages. Values represent the mean ± SD from at least three biological replicates. Statistically significant differences ($P<0.05$) between the control genotype and transgenic lines are marked with an asterisk.
209x303mm (300 x 300 DPI)

Figure 3

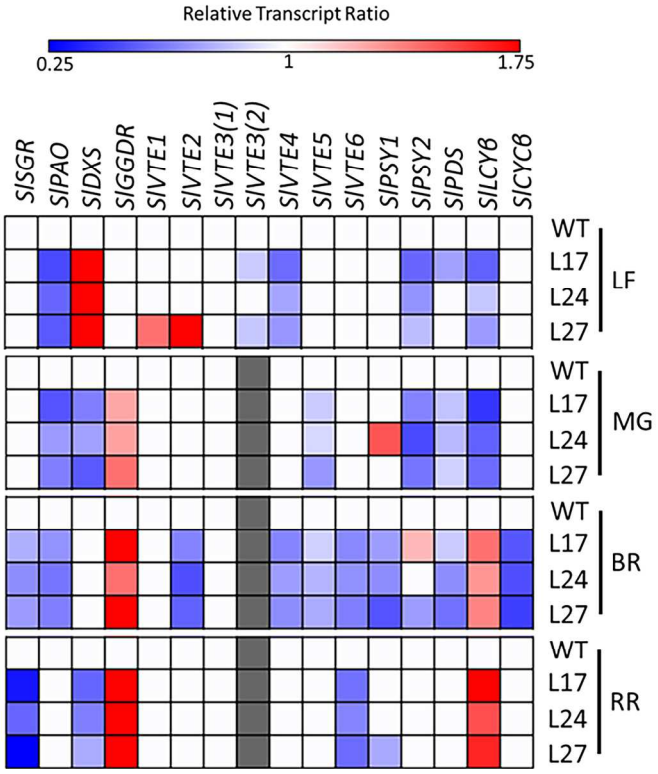

Fig. 3 Transcript profile of chlorophyll degradation, carotenogenesis and tocopherol biosynthetic genes in leaves and along fruit ripening of SlPPH-knockdown lines. Heatmap representation of the statistically significant ($P<0.05$) relative transcript amount compared to the corresponding wild type sample. The expression values are detailed in Supplementary Table S1. The abbreviations indicate: SlSGR, stay-green; SlPAO, pheophorbide a oxygenase; SlDXS, 1-deoxy-d-xylulose-5-P synthase; SlGGDR, geranylgeranyl diphosphate reductase; SlVTE1, tocopherol cyclase; SlVTE2, homogentisate phytyl transferase; SlVTE3, 2,3-dimethyl-5-phytylquinol methyltransferase; SlVTE4, tocopherol C-methyl transferase; SlVTE5, phytol kinase; SlVTE6, phytyl phosphate kinase; SlPSY, phytoene synthase; SlPDS, phytoene desaturase; SlLCYβ, chloroplast-specific β-lycopene cyclase; SlCYCβ, chromoplast-specific β-lycopene cyclase; LF, leaf; MG, mature green fruit pericarp; BR, breaker fruit pericarp; RR, ripe fruit pericarp. Values represent means from at least three biological replicates. SlVTE3(2) was not evaluated in fruits (grey boxes) because it is leaf-specific (Quadrana et al. 2013).
209x303mm (300 x 300 DPI)

Figure 4

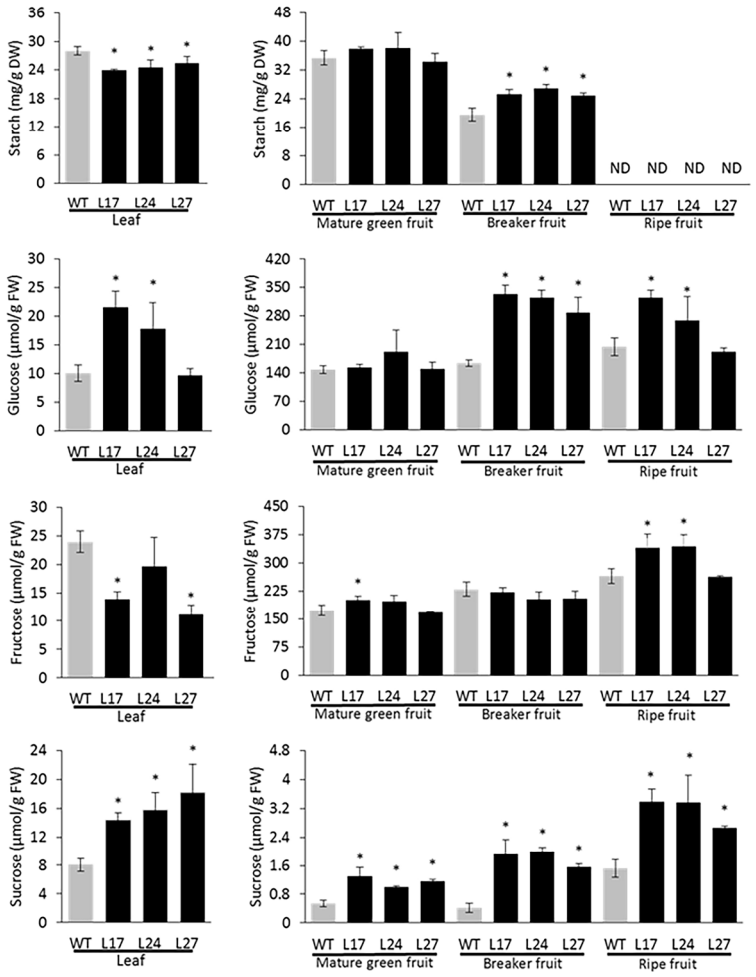

Fig. 4 Starch and soluble sugar content in SlPPH-knockdown lines. The content of starch and soluble sugars (glucose, fructose and sucrose) was measured in leaves and fruits at the mature green and ripe stages. Values represent the mean ± SD from at least three biological replicates. Statistically significant differences ($P<0.05$) between the control genotype and transgenic lines are marked with an asterisk.
209x303mm (300 x 300 DPI)

Figure 5

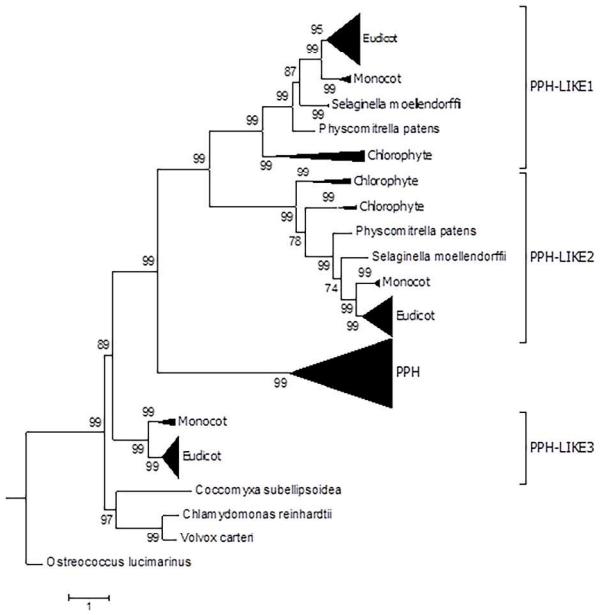

Fig. 5 Phenetic analysis of PPH homologous protein sequences. PPH homologs were identified in the Phytozome database (Supplementary Tables S4). Tree topology reveals four clades: the already functionally characterized PPH clade and three still uncharacterized clades that were named PPH-LIKE1-3.
205x297mm (300 x 300 DPI)

Figure 6

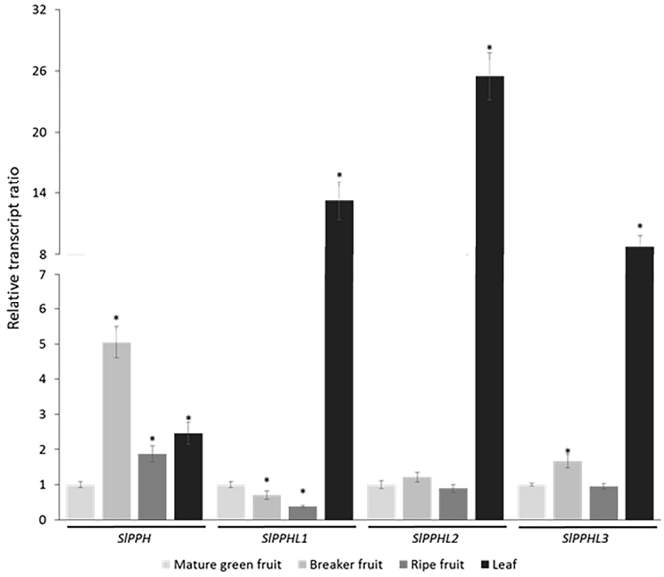

Fig. 6 Transcript profile of SlPPH and SlPPHLs genes in leaves and along fruit ripening of the wild type genotype. Data represent the mean ± SD from at least three biological replicates and are expressed as relative transcript amount compared to the corresponding mature green stage. Statistically significant differences ($P<0.05$) compared to the mature green stage are marked with an asterisk.
209x303mm (300 x 300 DPI)

Figure 7

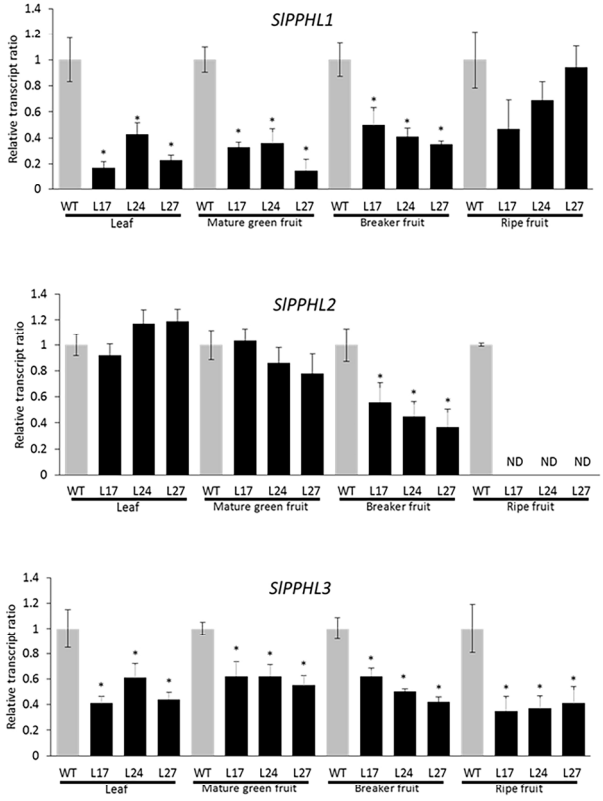

Fig. 7 Transcript profile of SlPPHLs in SlPPH-knockdown plants in leaves and along fruit ripening. Data represent the mean ± SD from at least three biological replicates and are expressed as relative transcript amount compared to the corresponding wild type sample. Statistically significant differences ($P<0.05$) compared to the mature green stage are marked with an asterisk.
167x297mm (300 x 300 DPI)